High Velocity Gas in the Line of Sight to the Vela SNR

Joy S. Nichols

Harvard-Smithsonian Center for Astrophysics, 60 Garden Street, MS 34, Cambridge, MA 02138

jnichols@cfa.harvard.edu

and

Jonathan D. Slavin

Harvard-Smithsonian Center for Astrophysics, 60 Garden Street, MS 34, Cambridge, MA 02138

jslavin@cfa.harvard.edu

1. Introduction

One of the best objects for study of the structure, kinematics, and evolutionary status of a middle-aged supernova remnant (SNR) is the VELA SNR, due to its proximity (approximately 250 pc, Jenkins & Wallerstein 1995, Cha & Sembach 2000), extensive optical filamentary structure, and an abundance of hot background stars for absorption line research. The VELA remnant is 7.3 degrees in diameter, based on x-ray imagery with ROSAT, with the pulsar nearly centered in the remnant (Achenbach et al. 1995). The western region of the remnant has much lower x-ray surface brightness than the remainder of the remnant and in fact escaped earlier detection with previous instrumentation. The remnant is believed to be about 11,000 years old (Reichley, Downs, & Morris 1970).

Several studies of the interstellar absorption line data in optical wavelengths have previously shown the presence of high velocity features to the Ca II and Na I lines (Wallerstein & Silk 1971; Wallerstein, Silk, & Jenkins 1980; Jenkins, Wallerstein, & Silk 1984; Hobbs 1991; Danks & Sembach 1995; Cha & Sembach 2000). which can yield important information concerning gas kinematics, morphology, abundances and depletions, Even more remarkable that the numerous high velocity features recognized by these studies is the recent discovery that the interstellar features, including the high velocity features, are time variable with time scales of a few years (Hobbs 1991; Danks & Sembach 1995; Cha & Sembach 2000).

High-velocity absorption components to the interstellar lines in ultraviolet data, which allow a much wider range of ionization potential and thus temperature, density, and pressure

mapping than are available in the optical wavelengths, were first reported by Jenkins, Silk, & Wallerstein (1976), who studied 4 stars in the VELA SNR line of sight using Copernicus data. These authors found velocities in the range of –90 km s^{-1} to +180 km s^{-1} with a possible component at –450 km s^{-1}. Jenkins, Wallerstein, & Silk (1984) studied absorption line profiles in IUE high dispersion data of 45 stars in the VELA SNR line of sight, finding high velocity components in more that one third of the program stars, with velocities up to +180 km s^{-1}. Their analysis of IUE data showed chaotic kinematics, no geometric effects of expansion, lower depletion than the normal interstellar medium (ISM), and some relatively strong lines of C I. Using emission line UV data, Raymond, Wallerstein, & Balick found evidence of a thermally unstable shock wave behind a 150 km s^{-1} shock. Their calculations also indicate the shock is nearly face-on.

While IUE high resolution data do not have the resolution of more current instrumentation, the large number of spectra available in the IUE archives provide an opportunity to map spatially the high-velocity components to the interstellar lines and compare the morphology of the hot gas to X-ray imagery. The IUE archive has been reprocessed with improved calibrations and image processing techniques, so that revisiting previously published results of earlier investigators is useful because of the reduced errors and comparablity of the spectra. The intent of this paper is to create a global survey of the high-velocity gas detected in the UV toward the VELA SNR. This paper describes a survey of 60 stars in the VELA region with an inventory of high-velocity features. In Section 2 we describe the nature of the study and the spectral data. The results of the velocity measurements toward the target stars for neutral species, low ionization, and high ionization lines are presented in Section 3. Section 4 is a discussion of the results as they relate to the interaction of the SNR shock with the ISM.

2. Observations

We are currently engaged in a survey of all high disperion IUE data of hot stars near the galactic plane with the goal of cataloging high-velocity components in the interstellar absorption lines. The project includes high ionization (C IV, Si IV, and N V) and low ionization (Fe II, C II, Si II, Al II, and S II) lines present in either SWP or LWP/R spectra of O and B stars. We have selected all stars in the IUE archive with $258 \leq l_{II} \leq 269$ degrees and $-8 \leq b_{II} \leq +2$ degrees for study of the VELA SNR. These stars are listed in Table 1, along with their galactic coordinates, Hipparcos distance estimates if available, spectral types, and IUE image sequence numbers analyzed. The positions of these stars is shown in Figure 1. While the sampling of the region is generally quite good, there are a few unsampled pockets

evident in the figure, particularly about 1 degree west and 1 degree east of the VELA pulsar. The lack of data in these regions must be considered in the conclusions to this work. The spectra used in this survey were processed with IUESIPS.

The radial velocity measurements of high-velocity features and the equivalent width of these components are reported in Table 2. These spectra were corrected to heliocentric velocities in the IUESIPS processing, or corrected for this study if necessary. Even after correction to heliocentric velocities, there are residual errors in each spectrum due to image distortion and spectra format motion. We would have preferred to add a correction to each radial velocity measurement which was determined from the mean of the neutral ion lines in the same spectrum as has been done in previous studies (Nichols-Bohlin & Fesen, 1986, 1993), but as noted below, the neutral C I (representing the majority of the available neutral ions in SWP spectra) are variable in wavelength and sometimes may high-velocity components of their own, making them unreliable fiducials in the VELA region. We therefore chose to report heliocentric velocities assigned in the processing or determined by us. The error in the velocities presented here is +/- 5km/s.

An important source of error in the radial velocities reported here. The long-wavelength spectrum of an object often has a velocity offset from the short wavelength (SWP) spectrum of the same object, based on the mean of the main interstellar components and in particular on the Fe II λ1608 line radial velocity in the SWP spectrum compared to the Fe II λ2382, 2585, 2599 lines in the LWR/P spectrum. This offset, which is generally about +17 km s^{-1} between the LWR/P spectrum and the SWP spectrum of the same object, has been previously reported (Nichols-Bohlin & Fesen 1986) but the source of the error remains unknown. Because the error is not always present, and SWP spectra analyzed here form a consistent group of main component velocities, we assume the error is in the long-wavelength assignments from IUESIPS, and have corrected these velocities such that the main components in the LWP/R spectrum match those in the corresponding SWP spectrum.

Another source of uncertainty in this study is the non-uniform time epoch. As Cha & Sembach (2000) have shown, the velocities and the equivalent widths of the interstellar line components in this region can vary of time scales of a few years (or less). While most of the spectra used in this study were taken during 1978-1979, a few were taken as late of the mid-1990's.

It was not always possible to measure all of the interstellar lines. For example, the C II line at 1334 Å is contaminated by a reseau mark in large aperture IUE spectra, discounting valid measurements. Al II lies at the end of an echelle order and the ripple correction for this order can be unsatisfactory, producing spurious features. Al III has not been included in this study because it is almost always includes a photospheric component for the spectral

type of the stars in this study. The data for Si II presented in the following tables include a summary of 4 lines (1260 Å, 1304 Å, 1506 Å, 1808 Å). Although the Si II lines at 1190 Å and 1993 Å were always examined, this region of the IUE echellogram is generally too noisy to make confident measurement. The main component, not reported in Table 2, generally lies at +7 - +17 km s^{-1} in the VELA direction.

The equivalent width of each high velocity feature was measured using an interactive tool provided by the IUEDAC. Two points on either side of the feature were selected to represent the continuum. These points were selected in regions at least .5 Å from the edge of the feature being measured, in a region devoid of any identifiable absorption or emission features. If it were assumed that the data represent the true continuum with no absorption or emission features, then the appropriate continuum level would lie halfway between the maximum and minimum flux values that represent the noise in the data. Since it is assumed there are still unidentified absorption features below the resolution of IUE, the continuum was chosen as approximately 0.4 (maximum data value - minimum data value) + minimum data value. The equivalent width is the total area below the selected continuum. The radial velocity of the line is represented here as the minimum extremum in the line center. This is not as accurate as a gaussian fitting technique, and the errors reflect the reduced accuracy. The intent of this work was to identify lines of sight that warrented future investigation, and gain a global view of the ionization and kinematics in the various lines of sight toward the Vela SNR.

2.1. Discussion of Individual Stars

HD 72014

The only high velocity components in the lower ionization lines are in C II. Both C II lines show components between -110 and -114 km s^{-1}. In addition, C II 1335Å shows a component at +50 km s^{-1}. The high ionization lines show a far richer array of high velocity features. A positive component between +124 km s^{-1} and +140 km s^{-1} is present in Si III, both members of the C IV doublet, and N V 1238Å. A component at +165 km s^{-1} is present in N V 1242Å. A negative component at -49 km s^{-1} is seen in Si IV 1402Å and in both members of the C IV doublet. There is also a possible component at -271 km s^{-1} in N V 1242Å.

HD 71216

High velocity component arre exclusively near -60 km s^{-1}. Generally, these components are blended with the main component. This is one of the few stars in this study that showed

high velocity gas in Mn II. No N V was detected, and the C IV and Si IV lines are weak and narrow. The main component was only detected in C IV 1548Å.

HD 71459

This is a B V star with many sharp absorption lines, most of which are probably stellar in origin. For this reason, the high velocity interstellar lines reported in the tables are considered questionable.

HD 71019

High velocity components are only seen in the lower ionization lines of C II. These lines are quite weak and have a velocity of -110 km s^{-1}. The high ionization lines of C IV, Si III, and Si IV show components at -50 km s^{-1} and +140km s^{-1}. The components reported in N V are not consistent with the -50km s^{-1} and +140km s^{-1} components (except perhaps the N V component at +165 km s^{-1}), and are not repeated in both members of the N V doublet.

HD 71336

This line of sight shows virtually no lower ionization high velocity features. The only one reported in the tables is in the C II 1335Å line, but would be contaminated by a reseaux mark in the C II 1334Å line. There are several components in the high ionization lines. The +110 km s^{-1} component is the most prevalent, appearing in C IV and N V. The main component in C IV is red-shifted by about +15 km s^{-1}. The +420 km s^{-1} component in C IV appears in both members of the doublet, as does the +110 km s^{-1} component. The remarkable - 792 km s^{-1} component is present in both members of the Si IV doublet. While there are no other components at this velocity in the line of sight to this star, components with similar velocities are present in the spectra of other stars in this study. The component at -1127km s^{-1} is very questionable because it only appears in the 1242Å component of N V. However, there are other components with a similar velocity in the spectra of other stars in this study, so it has been included.

HD 72179

A component at +125 km s^{-1} is present in C II and one line of Si II. This component is also seen in the strongest Fe II line at 2599Å. The Fe II lines also so a ver strong compoent at +80km s^{-1}. The -125 km s^{-1} component in the Fe II 2599Å must be considered questionable because it is not seen in any other line. The Mg II lines have a component at about +500 km s^{-1}, as does the Fe II 2599Å. Note that there is a component at +391 km s^{-1} in the C II 1335Å line; if present in the 1334Å line, it would be contaminated by a reseaux mark. There is a component at -117 km s^{-1} in the C IV 1548Å line. If present in C IV 1550Å, this component would be blended with the Fe III line, which is clearly seen.

HD 72067

There is no LWP/R observation of this star. There is a single measurement of high velocity components for the lower ionization lines at Si II 1526ÅThe Si IV lines show a questionable component at +100 km s^{-1}, although the component appears in both members of the doublet. The C IV doublet shows a component at -95 km s^{-1} and one at +255km s^{-1}, the latter being a questionable measurement. The N V component at -81 km s^{-1} is present in both members of the doublet and is consistent with the similar component in C IV.

HD 72127

There are only a few high velocity components in the spectra of this star. There is a component at +115 km s^{-1} in the Si II 1526Å line. There are also 2 components between -6 and -15 km s^{-1} in the Si II and C II 1335Å lines. Al II shows a component at -108 km s^{-1}. Fe II 2599Å has a component at +97 km s^{-1}, and Mn II shows a component at +54 km s^{-1}. In the high velocity lines, only N V shows evidence of high velocity components, with -90 km s^{-1} in 1238Å and +108 km s^{-1} in 1242Å. Overall, the velocities are not consistent with one another and are likely questionable because the spectral type of the star is B2 IV.

HD 72648

There is no LWP/R observation of this star. No high velocity components were detected in the lower ionization lines in the spectrum. The Si IV 1393Å line has 3 components, at -443, -237, and +503 km s^{-1}. In N V, there is a component between -123 and -149 km s^{-1} in both members of the doublet. A possible component at -719 km s^{-1} is also present in both lines. There is a component at +242 km s^{-1} in the 1238Å line.

HD 72350

The +140 km s^{-1} feature is present in Fe II 2585Å and 2599Å, Al II at 1671Å, as well as both members of the Mg II doublet. The Mg II doublet also show a component at +103 km s^{-1} and -117 km s^{-1}. Al II also has a component at -108 km s^{-1}. Other lower ionization components in the Si II lines appear somewhat random. The +140 km s^{-1} component is present in both members of the C IV doublet. A component at -111 km s^{-1} also appears in both members of the C IV doublet. The +640 km s^{-1} component appears in both members of the N V doublet.

HD 72088

A component between -40 and -55 km s^{-1} appears in Si II, C II, Al II,Fe II, and Mg II. In most cases, it is a blend with the main component. This component is also present in N V. There is also a component near 0 km s^{-1} in Mg II and Fe II 2599Å, which is also blended

with the main component. The C II doublet has a component in both members at +115 km s^{-1}, and the Mg II doublet has a component that could be related. A component at +40 km s^{-1} appears in Fe II 2382 and 2585Å, and the Mg II doublet.In the high ionization lines there is evidence for a component around -100 km s^{-1} (Si III, Si IV, C IV), and around +100 km s^{-1} (Si IV, C IV). The +42 km s^{-1} component in C IV 1548Å is consistent with components seen in Si II, Fe II, and Mg II.

HD 72089

A predominant component at about +80 - +90 km s^{-1} is seen in Si II, C II, Al II, Fe II, and Mg II. Another component at about -60 to -70 km s^{-1} is seen in Fe II and Mg II. A component at about +79 km s^{-1} is clearly seen in both members of the multiplet for C IV. The Si IV lines are not consistent; the stronger member of the multiplet has components at -141 km s^{-1} and +144km s^{-1}, while the weaker member has one component at -113 km s^{-1}, which should be considered questionable.

HD 72555

There is no LWP/R observation of this star. This is a B2 V star and confusion with stellar features is possible. None of the lower ionization lines show believable high velocity features. The Si IV line at 1393Å shows a component at -366 km s^{-1}. The C IV lines have a wealth of high velocity features, with the +378 to +390 km s^{-1} feature present in both members of the doublet.

HD 72997

There is no LWP/R spectrum of this star. Only one high velocity feature was detected in any interstellar line. N V 1238Å has a component at -58 km s^{-1}.

HD 74620

There is no LWP/R spectrum of this star. No high velocity components were seen in the lower ionization lines in this spectrum. Only the C IV lines showed high velocity components in the high ionization lines. Both members of the C IV doublet has a component between +388 and +408 km s^{-1}. Also, both lines have a component between -113 and -124 km s^{-1}. In addition, the C IV 1248Å line has a component at -319 km s^{-1}.

HD 74234

The only low ionization lines showing high velocity components are Fe II and Mg II. Fe II 2382Å has a component at +62 km s^{-1} and Fe II 2599 km s^{-1} has a component at +47 km s^{-1}. Both members of the Mg II doublet have a component at +67 km s^{-1}. In the high ionization lines, There is a component between +144 and +159 km s^{-1} in Si III, Si IV,

and C IV. Si III also shows a component at -139 km s^{-1} and one at +59 km s^{-1}. The C IV 1334Å line has a component at +91 km s^{-1}. All of these high ionization components have been indicated as questionable because of blending and the spectral type of the star, B2 IV.

HD 72531

There is no SWP spectrum for this star. The Fe II 2599Å line has components at -195 and -146 km s^{-1}. Fe II 2382Å has a single component at -176 km s^{-1}, which could be a blend of the two lines seen in the Fe II 2599Å line. Mg II 2795Å has a component at -154 km s^{-1}, as does Mn II at 2605Å.

HD 74530

The Si II lines and C II doublet have components at about -117 km s^{-1}. This velocity does not appear in a component for the Fe II or Mg II lines. Another component at about +70 km s^{-1} is present in Si II 1526Å, as well as two of the Fe II lines and the Mg II doubltet. The high ionization lines present a very different picture. A component about -130 km s^{-1} is present in Si III, Si IV, C IV, and N V. The only other detectable high velocity feature in the high ionization lines is a questionable component at -346 km s^{-1} in C IV 1548Å.

HD 74234

No high velocity components were seen in Si II or C II. Fe II has a component at +62 km s^{-1} in the 2382Å line, and at +47 km s^{-1} in the 2599 Å line. These are relatively strong components, with equivalent widths approximately 30-50% of the main components in each line. Mg II shows a component at +67 km s^{-1} in both members of the doublet. The high ionization lines show a wider range of velocities than the lower ionization lines. Si III has coomponents at -139, +59, and +144 km s^{-1}. Si IV shows a component in both members of the doublet between +126 and +144 km s^{-1}. C IV has a negative component between -334 and -345 km s^{-1} in both lines. There is also a component between +144 and +159 km s^{-1} in both lines. A single component at +91 km s^{-1} is seen in C IV 1548Å. All of the high ionization components are indicated in the tables as questionable. However, there is a clear consistence between the various ionization species, at least for the component at about +144 km s^{-1}. The Si III component at +59 km s^{-1} is consistent with the lower ionization components.

HD 74436

There is no LWP/R spectrum for this star. No high velocity components were seen in the lower ionization lines. In the high ionization lines, Si IV has a component at -136 km s^{-1} in the 1393Å line, and a component at -93 in the 1402Å line. C IV has a component between -112 and -122 in both members of the doublet. N V has a component between -48 and -61

km s^{-1} in both members of the doublet.

HD 74580

There is no LWP/R observation of this star. The low ionization components are spread over a range of -89 to -119 km s^{-1}. The questionable component at +117 km s^{-1} in C II 1334Å may be a blue-shifted component of C II 1335Å. However, the C II 1335Å line has a red wing. The red-shifted component to Fe II does not match any other velocity is this spectrum. In the high velocity lines, only the C IV lines show high velocity componets. The components, at about -85 km s^{-1} and +305 km s^{-1} are clear detections.

HD 74273

There is no LWP/R spectrum of this star. The lower ionization lines revealed no high velocity components. Only C IV in the high ionization lines showed high velocity features. There is a components between -118 and -129 km s^{-1} in both members of the C IV doublet. There is also a components between +139 and +158 km s^{-1} in both C IV lines, which is at least as strong as the main component.

HD 74662

There is no LWP/R spectrum of this star. The lower ionization lines have no high velocity features. In the high ionization lines, only Si II has such a feature, at -162 km s^{-1}.

HD 72754

Virtually all of the interstellar lines in this spectrum have red wings. While the measurements of high velocity features appeared certain, the inconsistency of the velocities among the various ionization species suggests the blending in the lines renders the velocity measurements suspect. The -1196 km s^{-1} feature in both members of the Mg II doublet may be contaminated by another Mg II transition. However, this velocity is evident in other spectra in this study so it is included.

HD 69648

Both members of the C II doublet show features at about -78 km s^{-1} and +44 km s^{-1}. No features were seen in the Si II, Fe II, or Al II lines. The Mg II doublet has high velocity features at about -73 km s^{-1}. The -78 km s^{-1} component is again seen in the Si II line, but not in the other high ionization lines. There are two components in the C IV lines, at -6 and +52 km s^{-1}, and a -15 km s^{-1} component in the Si III line. These are questionable because of the blending with the main component.

HD 69882

There is no SWP spectrum of this star. The interstellar lines are blended and lead to questionable measurements. There is a component between -91 and -104 km s^{-1} in Fe II 2382Å and both members of the Mg II doublet. There is also a component between -146 and -138 km s^{-1} in the Mg II doublet. A single positive velocity component was seen in Mn II 2576Å at +52 km s^{-1}.

HD 70309

There is no LWP/R observation for this star. The C II lines have a clear component at +72 km s^{-1}. The Si II 1526 km s^{-1} line has a componet at +91 km s^{-1}. There is also a +90 km s^{-1} component in the stronger member of the Si IV doublet, but the weaker member shows a component at +127 km s^{-1}. No high velocity components were seen in the C IV lines, and the main components of the C IV are comparatively weak and narrow. The two N V components at -113 and -67 km s^{-1} are only seen in the 1242Å member of the doublet.

HD 75759

The high velocity component seen in the spectra of this star between -3 and -23 km s^{-1} is always blended with the main component. This component is present in the C IV lines as well as the lower ionization lines. There is also a component at about +87 km s^{-1} in the C II lines only.

HD 76341

A few components at between -18 and -27 km s^{-1} are present in Si II and C II. The O I line at 1302Å also shows a component at -27 km s^{-1}. The Si III line has a clear blue wing.

HD 72537

There is no LWP/R observation of this star. The component in Si II at 1260Å may be spurious, but the main component at this line is red-shifted compared to the other main components in this spectrum. It may be that the other lines are blends of this -23 km s^{-1} feature and a red-shifted main component. This is a B3 V star and the wealth of spectral absorption features could confuse the results for this star. There is a component at +124 km s^{-1} in one Si II line and one member of the C II doublet. The two components of Al II are also seen in Al III 1862Å.

HD 72798

The Si II lines at 1190Åand 1193Å both show a component at about -360 km s^{-1}, which is not reported in the tables because most spectra have insufficient flux in this wavelength region for a measurement of lines. A component at about +75 km s^{-1} is seen in one line of Si II, C II 1334Å, and Mn II. Another component at about +110 km s^{-1} is seen in one Si II

line, one Fe II line, both lines of the C II doublet, and both members of the N V doublet. The component at -234 km s^{-1} in C II is not seen in other lines. But the questionalble components of +373 and -500 km s^{-1} in C II 1335Å may be real. There is a component at about +400 km s^{-1} in both C IV lines. Several negative components were also seen in the high ionization lines, including a component around -800 km s^{-1} in Si IV, and a component at -111 km s^{-1} in the same lines. The N V shows a component at -80 km s^{-1}.

HD 74319

This is a B3 V star which is expected to have many stellar absorption lines that could confuse the results. However, the component velocities measured are very consistent and lend credibility to the measurements. The primary high velocity component is at abou -50 km s^{-1}, present in Si II 1808Å (the other Si II lines are very strong and saturated), Al II, Fe II, and C IV. The Mg II lines show a blue wing, but are saturated. The Fe II lines at 2382 and 2585Åmay be due to confusion with stellar features.

HD 73010

There is no LWP/R spectrum of this star. No high velocity components to the interstellar lines were detected in the lower ionization lines. In the high ionization lines, C IV has a component between -108 and -118 km s^{-1} in both members of the doublet. N V has a component at -131 km s^{-1} in the 1242Å line only.

HD 74194

There is no LWP/R spectrum for this star. There are two components at about -60 km s^{-1}, one in Si II and one in C II 1335Å. C II 1334Å shows components at -163 and -29 km s^{-1}. In the high ionization lines only Si III has evidence of high velocity features, with components at -141 and -53 km s^{-1}.

HD 74195

There are only 2 detections of high velocity components in the lower ionization lines. Fe II 1608Å has a component at -138 km s^{-1}, and Fe II 2599Å has a component at -115 km s^{-1}. In the high ionization lines, a component at -78 km s^{-1} was detected in N V 1238Å.

HD 75149

There is no LWP/R spectrum for this star. One the whole, the interstellar lines in the SWP spectrum are very broad and it was difficult to sort out specific high velocity features. The positive velocity features reported in the Si II lines range between +113 and +143 km s^{-1}. These velocities indicate a red-shifted component, but the velocities are questionable. The N V doublet shows a feature at +116 km s^{-1}, but other high ionization lines have no detectable

high velocity features.

HD 74753

High velocity components were only seen in the high ionization lines. Si IV has two components in both members of the doublet. One component is between -324 and -357 km s^{-1}. The other component is between +869 and +887 km s^{-1}. N V 1238Å has a component at -198 km s^{-1}. N V 1242Å has a component at -116 km s^{-1}.

HD 67621

There is no LWP/R spectrum for this star. Only one high velocity component was detected. Both members of the C IV doublet have a component at -103 to -107 km s^{-1}.

HD 70084

There is no LWP/R spectrum of this star. The lower ionization lines showed no high velocity components to the interstellar lines. In the high ionization species, C IV has a component between -94 to -106 km s^{-1}in both members of the doublet. N V has a component at -79 km s^{-1} in the 1238Å line.

HD 70930

There is no LWP/R spectrum of this star. No high velocity features were detected in the lower ionization lines. In the high ionization lines, Si IV could not be measured because it was in the trough of broad absorption. C IV showed 3 components in both members of the doublet. There is a component between -107 and -118 km s^{-1} a component between -49 and -59 km s^{-1} and a component between +18 and +28 km s^{-1} in both lines. The small positive component is probably the red-shifted main component, as is often seen in the high ionization lines.

HD 76566

There are a number of negative components between -100 and -140 km s^{-1}, including Si II, C II, and Fe II. There is also a similar component in Si II 1193Å at -124 km s^{-1}. The Si II line at 1194.5Å has a component at -1015 km s^{-1}. A positive velocity component is seen in 2 lines of Si II at about +93 and +120 km s^{-1}, respectively. The negative component in Mg II at -159 km s^{-1} is weak and only seen in the stronger member of the doublet. One the whole, there are many absorption lines in this B3 IV spectrum, which makes the identification of interstellar components difficult.

HD 74773

There is no LWP/R spectrum for this star. No lower ionization lines show evidence of

high velocity features. Only C IV in the high ionization lines has high velocity features. A component at +339 to +343 km s^{-1} is present in both members of the C IV doublet. A component at +89 to +101 km s^{-1} is also present in both lines, as is a component at -67 to -72 km s^{-1}. A single questionable component at +317 km s^{-1} is seen only in C IV 1548Å.

HD 74711

There is no LWP/R spectrum for this star. There are very few high velocity components in the lower ionization lines. The +108 km s^{-1} component reported in the table for C II 1334Å may instead be a negative velocity component to the C II 1335Å line at -159 km s^{-1}. By contrast, the high ionization lines show a rich array of high velocity components. Both Si IV and C IV have negative velocity components at approximately -120 km s^{-1}. Also, Si IV and C IV have a component between +86 and +101 km s^{-1}. Both the Si II at 1190Å and 1193Å have components at about -415 km s^{-1}, which are not reported in the table. The N V component at -85 km $s^{-1}$is very broad, detected in only the N V 1238Å line. A component at +240 km s^{-1}, seen only in N V 1242Å is also seen in Si IV. The very high negative velocity components in C IV are at a velocity seen in other spectra in this study, although the detection of features at such high displacements is questionable.

HD75309

There is no LWP/R spectrum of this star. The Si II lines have a component at -76 km s^{-1} in two lines, with -52 km s^{-1} and -123 km s^{-1} seen in the other two lines. The C II doublet lines both show components at about +386 km s^{-1}In addition, the C II 1334Å line has components at -250 km s^{-1}, -37 km s^{-1} and +184 km s^{-1}. The C II 1335Å line also has a component at +229 km s^{-1}. In the high ionization lines, C IV has a component at -76 km s^{-1} in both lines, a consistent velocity with the Si II lines. The Si IV lines show a component at about +20 km s^{-1} in both lines. Si III has a component at +45 km s^{-1}, but the line is very broad and may be heavily blended with several components. N V has a component at -92 km s^{-1} in the 1238Å line, and a component at +93 km s^{-1} in the 1242Å line.

HD 75821

A negative velocity component at -73 to -95 km s^{-1} is pervasive in the low ionization lines. This component appears in 4 Si II lines, including 1193Å not reported in the table, both C II lines, Al II, 3 Fe II lines, and both Mg II lines The component is always relatively strong and unmistakable. In addition, a positive velocity component at ++81 to +89 km s^{-1} is seen in 2 Si II lines, one Fe II line, and both Mg II lines. The +110 km s^{-1} component in C II is also strong. There is no contamination of the C II 1334Å line by a reseau mark in this spectrum because it is a small aperature observation. The velocities of the high ionization

lines are somewhat different than the lower ionization lines. The -76 km s^{-1} component in Si III is similar to the components seen in the lower ionization lines, but there is also a very strong component at +132 km s^{-1}The components in Si IV at +18 to +27 km s^{-1} are actually the main component, displaced by blending or other phenomenon. The C IV lines have components between +102 to +120 km s^{-1}Also, C II 1335Å has a component at +145 km s^{-1}. As an additional note, the Mg I 2853Å line has a high velocity component at -79 km s^{-1}.

HD 77366

The Si II lines have a blue wing, which yielded measurements of a component in two of the lines. These measurements are questionable and not consistent in velocity. The Fe II 2599Å, Mn II 2605Å, and both Mg II lines show components between -40 to -51 km s^{-1}, although these also are blends. It is noted that is is rare in this dataset to see high velocity features in the Mn II lines. In the high ionization lines, only C IV has a high velocity feature: between -36 to -43 km s^{-1}, which is consistent with the Mg II features.

HD 77581

There is a negative velocity feature at -226 to -255 km s^{-1} in one Si II line, both C II lines, and Al II. A feature in Fe II 1608Å at -241 km s^{-1} may be related, but the lack of similar features in the stronger Fe II lines makes this feature questionable. There are several other negative velocity features in Si II and Al II, in the range of -20 to -58 km s^{-1}. By contrast to the negative velocities in the lower ionization lines, the high ionization lines have only positive velocities. Si IV has a component between +43 and +50 km s^{-1} in both lines. The only other high ionization line showing high velocity is N V 1238Å at +178 km s^{-1}

2.2. Low Ionization Discussion

The stars exhibiting high velocity features in low ionization lines are listed in Table 2 along with the velocity displacement for each of the singly ionized species and the equivalent width of the feature. While it is clear from these data that the lines of sight intersect multiple cooling regions, it is also clear that these regions are quite patchy and stars separated by as little as 1 pc show different velocity structures.

We find a concentration of components at -90 km s^{-1} and +120 km s^{-1}. There are two stars with a component at +400 km s^{-1} and two stars with a component at +500 km s^{-1}. There are also apparent components at +150 km s^{-1} and -140 km s^{-1}. The occurance of these features appears to be random across the VELA SNR in the region sampled by the

program stars and geometric effects are not clearly evident, although they may be present in the components with radial velocity $\leq$ 100 km s^{-1} seen in a number of the stars. However, these lower velocity components are not confined to the outer regions of the VELA remnant and cannot be exclusively attributed to the lower velocities expected when viewing the edge of a shell as opposed to the center. These lower velocities may indeed represent an additional structure to the obvious one at v = 100-120 km s^{-1} and v = 400-500 km s^{-1}.

2.3. Si IV Discussion

There are far fewer high-velocity components to the Si IV lines (total of 19 in our sample) than are present in either the low ionization lines (39 in our sample) or in the C IV data (56 in our sample). The components at -100 km s^{-1} and +120 km s^{-1} are again the most common, with the +150 km s^{-1} components also well represented. In addition, two components are present at -225 to -250 km s^{-1} and two components at -800 km s^{-1}. There is one component at -420 km s^{-1} and one at -350 km s^{-1}. While components present in only one spectrum are viewed as questionable, these two components have counterparts in the low ionization data (-400 km s^{-1}) and in the C IV data (-350 km s^{-1}).

2.4. C IV Discussion

The C IV high-velocity features are remarkable for their high frequency of incidence. Figure 2 is a plot of the positions of the stars with high-velocity C IV features detected in the spectra. As in the cases of the low ionization lines and the Si IV lines, the -100 km s^{-1} and +120 km s^{-1} components dominate the statistics, with the +150 km s^{-1} also well represented. Here we see the strongest evidence for additional high-velocity structures. The v = +400 km s^{-1} components are clearly identifiable as a distinct structure, with 4 stars showing this component. The component at -325 km s^{-1} to -350 km s^{-1} is also well defined, with 4 stars exhibiting these components. This set of components, like the [-100,+120] set, indicate a shell of cooling material expanding in VELA about the systematic velocity of +20 - +30 km s^{-1}, although, again, no geometric efects are clearly seen. There are also components at -230 km s^{-1} and +350 km s^{-1}, which may be statistically significant.

3. General Discussion

3.1. Distance

This study supports the proposal by Jenkins & Wallerstein (1995) that the distance to VELA should be revised. The distance of 400-500 pc had been accepted, primarily because of the presumed association between VELA and the Gum Nebula. Jenkins suggested that VELA is at 250 pc due to energy considerations. Two the the stars in this study which show high velocity components have distance estimates of 320 and 360 pc, respectively. In addition to strong C I*, these 2 stars show high velocity components in both low and high ionization lines, most of which are positive velocity components. Thus, a revised distance of 200-300 pc for VELA SNR would be consistent with our data. Cha et al. (1999) determine a distance to the Vela SNR of 250 $\pm$ 30 pc based on high resolution Ca II and Na I absorption line data and the Hipparcos distances to the stars. Our data indicate that the star with the smallest distance showing high velocity UV absorption lines is HD 71459 at a distance of 249 pc. The distance determined by Cha et al. is confirmed with these data.

3.2. Optical Filaments

The high velocity components detected do not show a clear geometric pattern expected from an expanding shell. At first glance, the velocities appear random and patchy. The lack of geometric pattern expected from an expanding shell has also been noted in other investigations of high velocity gas. To better understand the velocity structure of the Vela SNR, we have estimated the expansion velocity along each line of sight that would be expected from a symetrically expanding spherical shell. We have chosen a shock velocity of 165 km/s (Raymond) and a radius of the shell of 3.2 pc, based on the shell radius seen clearly in IRAS data. The shock velocity could be in error by 15 km/s, and the radius of the shell could be somewhat larger, so the line-of-sight expansion velocities we have determined could have an error of 15 km/s. Also we would expect the cooling regions behind the shock where the single to triple ionized species we have detected are formed to have the a lower expansion velocity as the shock itself. We have therefore identified all high-velocity components detected along each line of sight that are less than the expected line of sight expansion velocity +15 km/s as being potentially associated with the expanding shock. Only a few of the high velocity components we detected meet the test of geometric consistency with the expanding SNR shell.

When we eliminate the high velocity components that could potentially be due to the geometric expansion of the SNR, we are left with many components with velocities that are

disallowed based on expansion of the shell. Other authors have suggested that the are several sites of explosions within the remnant that could account for these high velocity components.

When the stars showing disallowed high velocity components are plotted on the [O III] image of the Vela SNR, a remarkable correlation is seen. Figure 3 is the [O III] image created from a collage of 4 images from the PGK atlas. Unfortunately, the images are not available electronically, so it was not possible to correct for background variations among the 4 individual images. But the strong filamentary structures are clearly visible. There is a polygon that is nearly symmetric around the pulsar position. We find that almost all the stars that show disallowed high velocity components lie along the filaments that define this structure. This is too great a coincidence to be ignored. We believe the [O III] structure is directly related to the high velocity features we have detected in low and high ionization species.

The high-velocity features detected coincident with the [O III] filaments suggest the structure is cylindrical and rotating. Only in this case would we detect radial velocity components only near the edges. Lines of sight through the center of the cylinder would have a small or no radial velocity component and a larger tangential velocity component.

We propose that the cylindrical structure seen in the [O III] image and defined by the high-velocity components is the signature of a cocoon formed by relativistic jets originating in the Vela pulsar. The northern jet is clearly seen in Chandra data.

The cocoon appears to be open-ended in both directions. In the north bright X-ray emission is seen at the top of the cocoon. Hot dust is also detected at the northern extent of the cocoon. In the [O III] image the northern edge of the cocoon shows intersecting arcs of emission.

The cocoon, however, does not appear to have a circular cross-section. The east-to-west filaments that define the northern and southern edges of the cocoon appear as straight lines. This would only be reasonable if the cocoon were very nearly in the plane of the sky, with no tilt toward the observer. But in this case one would expect to see a rectangle. We suggest that there has been a temperal change in the direction of the relativistic jet, such that the originaly the jet was directed very nearly north-south, and had a larger velocity that it currently does. Over time, the jet direction as moved so that it is now directed northwest-southeast, with a somewhat slower velocty. This scenario could produce the flattened cocoon with the east-west asymmetry. Currently, the northern jet as seen in Chandra data is generally oriented 45 °northwest, The temperal change is reinforced by the high-velocity features which appear primarily in the northwest and southeast edges of the cocoon as seen in [O III].

3.3. Global Mapping

We can conclude from the measurements of high velocity components to the ionized species that the structures responsible for the high velocity gas are patchy because detections, at IUE's resolution, vary over distances as short as a few parsecs. The velocity mapping does not appear to be a single shell expanding uniformly from the center of VELA due to the lack of geometric effects. The patchy, non-uniform expansion was also noted by Jenkins. Danks & Sembach (1995) suggest that some of the high-velocity gas in Vela may be accelerated by events other than the Vela SNR, based on the wealth of components seen in the spectra of member stars of IC2395, situated in the line of sight to the southeastern edge of the Vela x-ray perimeter. This is a somewhat confusing result because if the high- velocity features arise in the cooling gas behind the supernova shock wave, the velocities in this region should be near zero, yet the velocities are consistent with those seen near the center of the remnant. This situation prompted Danks & Sembach to suggest that some of the high- velocity gas in Vela may be due to events other than the original supernova. Even considering the later identifications of additional centers of explosions besides the Vela supernova itself (Vela Jr. and IC2395), the velocity mapping is more suggestive of many small structures rather than one, or a few, centers of expansion. The detection of multiple velocity components and lack of global geometric effects leads us to conclude that there are pre-existing clouds overrun by multiple shocks, providing multiple shock/cloud interfaces within the SNRs.

Considering the distances of the stars studies, we find the various high-velocity components may originate in spatially distinct regions. For stars with distance estimates less than 580 pc, only the –90, +120, and +150 km s^{-1} components are seen in all measured ionization states. The +400 and +500 km s^{-1} components appear in stars with distance estimate $\geq$ 580 pc. This would imply that the higher velocity components are formed in a different, background structure to the lower velocity components. The distance to the Gum Nebula is about 500 pc, and it is concievable that some of the high-velocity components arise in the Gum Nebula rather than the Vela SNR. However, we find no evidence for such high-velocity components in stars outside the Vela region. Edgar & Savage (1992) find high velocity gas associated with the Gum Nebula up to +80 km s^{-1}, based on the broad wings of the lines. So it seems unlikely that the higher velocities ($\geq$100 km s^{-1}) we measure are associated with the Gum Nebula, at 500 pc distance.

The distribution of high-velocity components suggests the most prevalent components (–90, +120, +150 km s^{-1}) are global in the Vela SNR and perhaps associated with the cooling interface behind the shock wave of the supernova. The higher velocity components (+400, +500 km s^{-1}) are less uniformly distributed but still cover the entire projected SNR. Other components occur in more localized regions. These components could be interpreted

as conductive cloud interfaces.

4. Conclusions

- The high-velocity components detected in the line of sight to the Vela SNR are not consistent with a single expanding shell of gas, but rather with multiple cooling interfaces within the SNR. These cooling interfaces may be multiple dense clouds within the SNR, and/or precursor structures.

- The range of velocities detected in the high-velocity components toward the Vela SNR are very large, ranging from -400 to +400 km $s^{-1}$and perhaps more. Only the Carina Nebula region in our Galaxy exceeds the range of detected high-velocity gas.

- Most of the lines of sight where high-velocity gas was detected lie along the periphery of a filamentary [O III] emission structure that is apparently cylindrical with a dimension of almost 8 degrees. This structure bisects the projected Vela SNR, and may be related to a previous stage of the precursor evolution.

References

Ashenbach, B., Egger, R., & Trumper, J. 1995, Nature, 373, 587.

Aschenbach, B. 1998, Nature, 396, 141.

Cha, A., Sembach, K., & Danks, A. 1999, ApJL, 515, L25.

Cha, A. N. & Sembach, K. R. 2000, ApJS, 126, 399.

Cha, A. N., Sahu, M. S., Moos, H. W., & Blaauw, A. 2000, ApJS,

Danks, A. & Sembach, K. 1998, AJ, 109,2627.

Edgar, R. & Savage, B. 1992, ApJ, 396, 124.

Hobbs, L. M., Ferlet, R., Welty, D. E., & Wallerstein, G. 1991, ApJ, 378, 586.

Ikeda, M., Oka, T., Tatematsu, K., Sekimoto, Y., & Yamamoto, S., 2002, ApJS, 139, 467.

Jenkins, E. B., Silk, J., Wallerstein, G., & Leep, M. 1981, ApJ, 248, 997.

Jenkins, E. B., Wallerstein, G., & Silk, J. 1984, ApJ 278, 649.

Jenkins, E. B. & Wallerstein, G. 1995, ApJ, 440, 227.

Jenkins, E. B., Tripp, T. M., Fitzpatrick, E. L., Lindler, D., Danks, A. C., Bech, T. L., Bowers, C. W., Joseph, C. L., Kaiser, M. E., Kimble, R. A., Kraemer, S. B., Robinson, R. D., Timothy, J. G., Valenti, F. A., & Woodgate, B. E. 1998, ApJL, 492, L147.

Koo, B. & Moon, D., 1997, ApJ, 485, 263

Koyama, H. & Inutsuka, S. 1999, in "Star Formation, 114.

Moriguchi, Y., Yamaguchi, N., Onishi, T., Mizuno, A., & Fukui, Y. 2001, PASJ, 53, 1025.

Reichley, P. E., Downs, G. S. & Morris, G. A. 1970, ApJ, 159, L35.

Smith, M. A., 2001, PASP, 113, 882.

Wallerstein, G., & Silk, J. 1971, ApJ, 170, 289.

Wallerstein, G., Silk, J., & Jenkins, E. B. 1980, ApJ, 240, 834.

Table 1. Stars Observed in the Vela SNR Region

Star	ra J2000	dec J2000	Spec. Type	distance Spect.	distance Hipparcos	SWP	Obs. Date
HD 68243	08 09 29.33	-47 20 43.0	B1 IV	400	···	32408	11/27/99
HD 68273	08 09 31.95	-47 20 11.7	WC	···	$258_{+41,-31}$	43022	11/06/91
HD 69404	08 14 51.24	-46 29 09.2	B3 Vnne	376	$408_{+127,-78}$	05534	06/15/79
HD 69648	08 16 02.74	-44 19 21.7	O8.5 Iab:	3602	···	25707	04/17/85
HD 69973	08 17 19.58	-47 55 12.3	B5 Vn	335	$417_{+132,-81}$	05511	06/13/79
HD 70084	08 18 01.15	-47 05 30.7	B7 III	501	$389_{+129,-77}$	20860	08/31/83
HD 70309	08 19 05.58	-48 11 52.3	B3 V	374	$253_{+40,-31}$	05530	06/15/79
HD 70930	08 22 31.69	-48 29 25.4	B1 V	348	$463_{+166,-97}$	05531	06/15/79
HD 71019	08 23 25.23	-42 48 26.2	B3 II/III	···	···	09434	07/03/80
HD 71216	08 24 35.28	-40 44 49.2	B5 Vn	448	$441_{+140,-86}$	20191	06/11/83
HD 71336	08 25 06.98	-43 21 52.7	B3 V	724	···	09433	07/03/80
HD 71459	08 25 51.91	-42 09 11.1	B3 V	242	$249_{+36,-27}$	05533	06/15/79
HD 72014	08 28 52.06	-42 35 14.9	B3 Vnne	400	$926_{+860,-301}$	05495	06/11/79
HD 72067	08 29 07.57	-44 09 37.5	B2 V	···	$490_{+219,-115}$	29376	10/05/86
HD 72088	08 29 12.64	-44 53 05.6	B3 III/IV	1630	···	38714	05/01/91
HD 72089	08 29 06.97	-45 33 26.9	B5 II/III	···	···	14096	05/28/81
HD 72127A	08 29 27.00	-44 43 30.0	B2 IV	230	···	43030	11/08/91
HD 72179	08 29 37.73	-44 05 58.0	B4 II/III	1574	···	14117	05/30/81
HD 72230	08 29 51.24	-44 44 36.0	B9 V	···	···	14118	05/30/81
HD 72350	08 30 39.23	-44 44 14.4	B4 V	281	$685_{+581,-216}$	44774	05/25/92
HD 72537	08 31 36.69	-45 47 05.2	B3 V	···	$377_{+104,-66}$	05529	06/15/79
HD 72555	08 31 39.65	-47 14 27.7	B2.5 V	590	$394_{+111,-71}$	05555	06/17/79
HD 72648	08 32 18.99	-43 55 53.4	B1/B2 Ib	3178	$741_{+708,-243}$	14126	05/30/81
HD 72754	08 32 23.38	-49 36 04.8	B2 Ia:pshe	···	$690_{+545,-182}$	05888	09/22/79
HD 72798	08 33 01.86	-45 45 10.	B3 III	···	$752_{+530,-220}$	14102	05/28/81
HD 72997	08 34 08.14	-44 32 41.4	B2 II/III	2173	$621_{+454,-184}$	05549	06/17/79
HD 73010	08 34 11.12	-45 38 11.7	B5 V	···	$746_{+683,-241}$	05550	06/17/79
HD 73882	08 39 09.53	-40 25 09.3	O8 V:	968	$500_{+719,-186}$	38311	03/06/90
HD 74194	08 40 47.79	-45 03 30.2	O9	2213	(2777)	05527	06/15/79
HD 74234	08 40 53.40	-48 13 31.8	B2 V	677	$629_{+351,-166}$	05491	06/11/79
HD 74273	08 41 05.32	-48 55 21.6	B1.5 V	519	$4230_{+219,-115}$	05494	06/11/79
HD 74319	08 41 34.90	-44 59 30.9	B3 V	394	$402_{+113,-73}$	05505	06/13/79
HD 74436	08 42 07.55	-48 14 40.8	B3 V	786	$412_{+523,-148}$	05525	06/15/79
HD 74530	08 42 36.55	-48 04 30.9	B3 IV/V	1226	···	05487	06/11/79
HD 74580	08 42 53.07	-48 07 41.2	B3 V	872	···	05488	06/11/79
HD 74620	08 43 07.03	-47 41 12.9	B4	907	···	05504	06/13/79
HD 74662	08 43 18.80	-48 20 42.9	B3 V	1008	···	05526	06/15/79

Table 1—Continued

Star	ra J2000	dec J2000	Spec. Type	distance Spect.	distance Hipparcos	SWP	Obs. Date
HD 74711	08 43 47.51	-46 47 56.4	B2 III	1004	···	14125	05/30/81
HD 74753	08 43 40.27	-49 49 22.1	B0 IIIn	977	$465_{+168,\ -97}$	05557	06/17/79
HD 74773	08 44 09.71	-47 06 58.0	B3 IV	735	$840_{+799,-275}$	05553	06/17/79
HD 74920	08 45 10.34	-46 02 19.2	O8	3130	···	05559	06/17/79
HD 75129	08 46 19.41	-47 32 59.6	B5 Ib	1725	$503_{+182,-106}$	14123	05/30/81
HD 75149	08 46 30.55	-45 54 45.0	B3 Ia	1780	$1010_{+12127-356}$	07726	01/21/80
HD 75309	08 47 27.97	-46 27 04.0	B2 Ib/II	3170	···	14124	05/30/81
HD 75549	08 49 03.36	-43 45 40.4	B3 V	556	$330_{+87,-57}$	14104	05/28/81
HD 75759	08 50 21.02	-42 05 23.2	O9 V	929	$585_{,+262,\ -139}$	06397	09/05/79
HD 75821	08 50 33.46	-46 31 45.1	B0 III	964	$826_{+623,-248}$	05560	06/17/79
HD 76161	08 52 38.61	-48 21 32.8	B3 Vn	296	$333_{+70,-49}$	06635	09/26/79
HD 76341	08 54 00.61	-42 29 08.8	O9 III	1471	$1220_{+3780,-526}$	28157	04/12/86
HD 76534	08 55 08.71	-43 27 59.9	B3 Vne	271	$412_{+473,-144}$	47830	06/08/93
HD 76536	08 54 59.17	-47 35 32.7	WC		(3448)	10113	09/13/80
HD 76566	08 55 19.20	-45 02 30.0	B3 IV	189	$287_{+60,-43}$	14121	05/30/81
HD 78616	09 07 42.52	-44 37 56.8	B2 II/III	1265	(1250)	10804	12/12/80

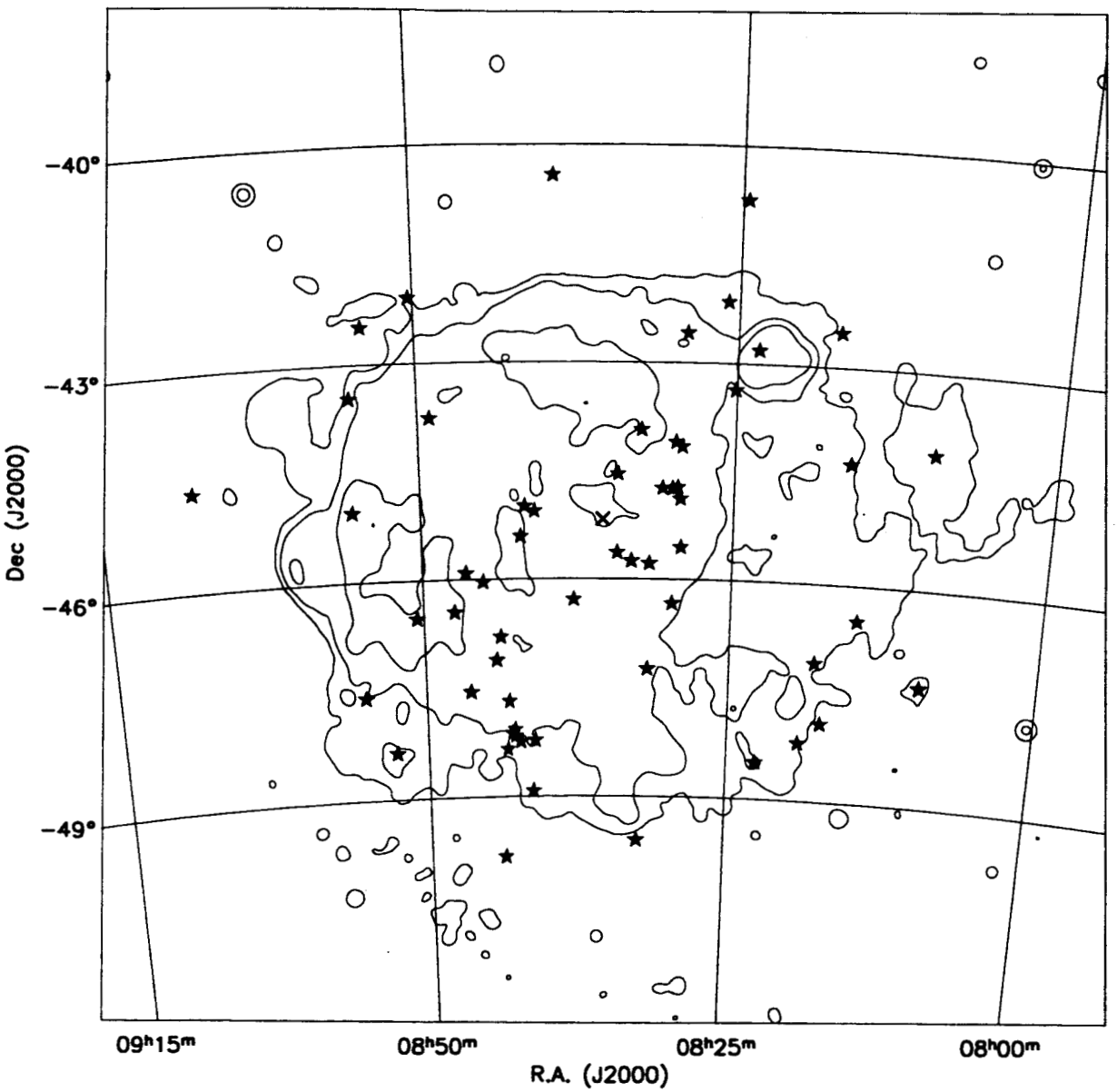

Fig. 1.— X-ray contours derived from the ROSAT all-sky survey image of the Vela SNR with all of the stars observed with IUE in this region overplotted. The position of the Vela pulsar is indicated with an "x" symbol.

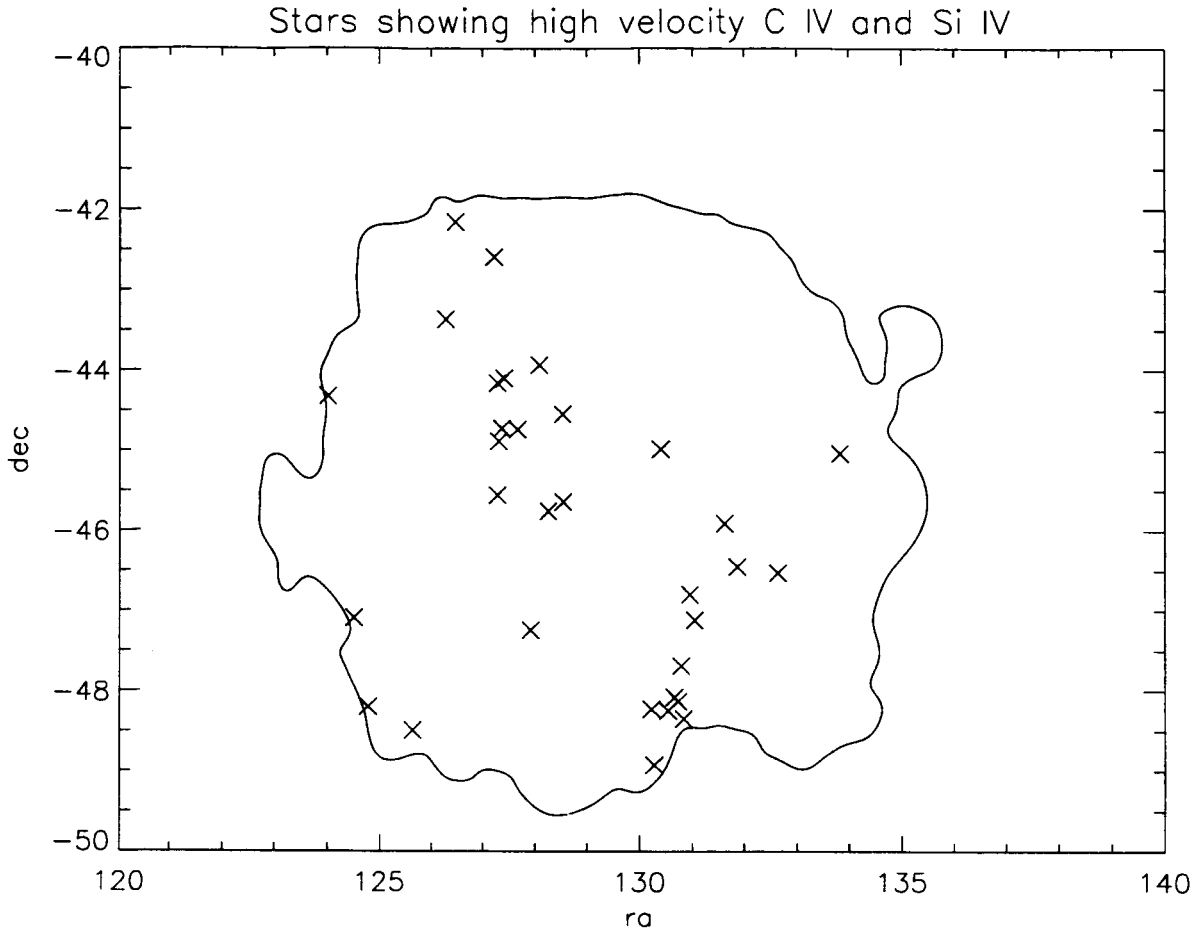
Stars showing high velocity C IV and Si IV
−40
−42
−44
−46
−48
−50
dec
120
125
130
135
140
ra

FIGURE 2

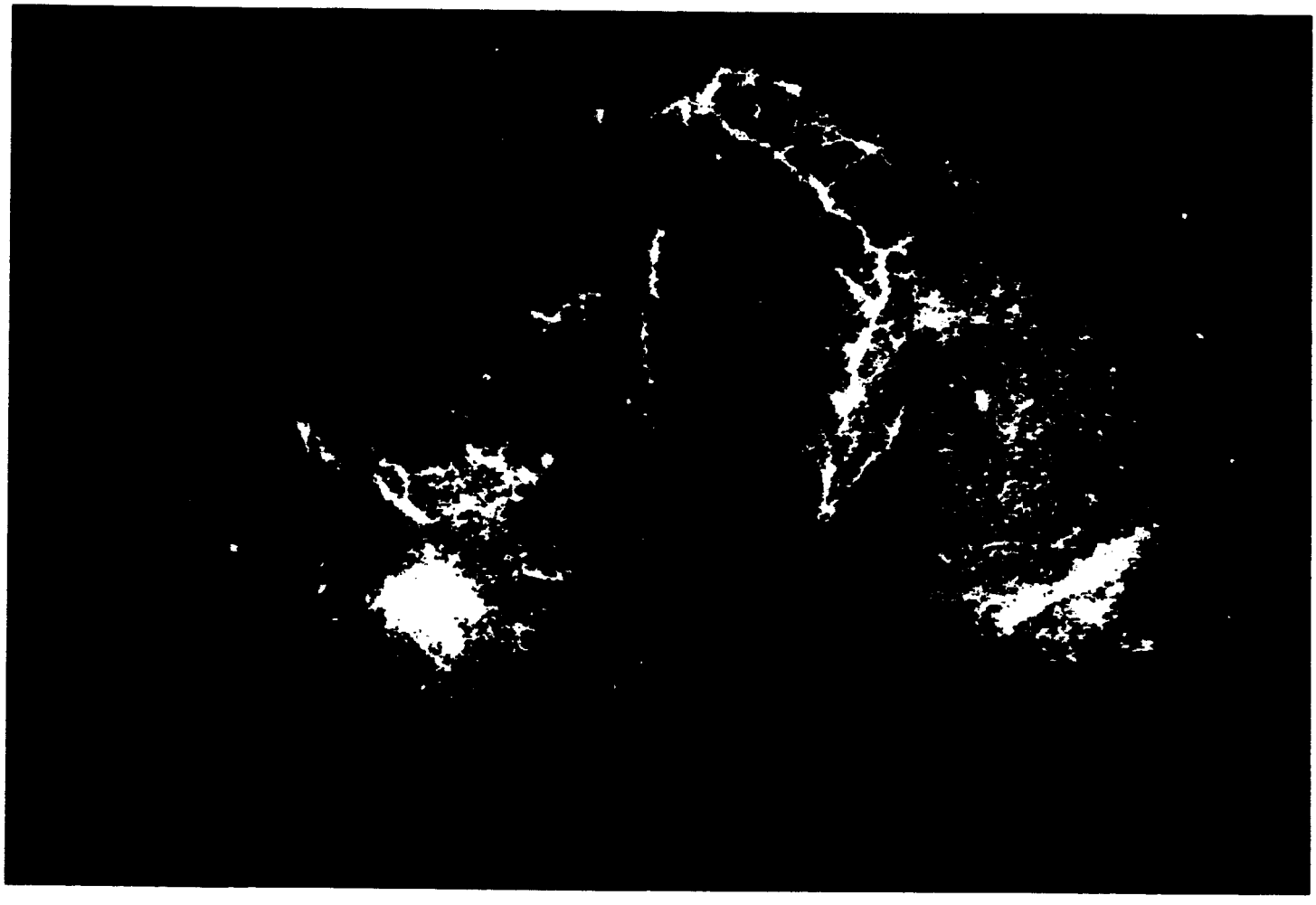

FIGURE 3.
VELA SNR IN [O III] λ5007. FIGURE IS CONSTRUCTED FROM 4 SEPARATE PLATES.